

COLOUR NORMALIZATION OF FUNDUS IMAGES BASED ON GEOMETRIC TRANSFORMATIONS APPLIED TO THEIR CHROMATIC HISTOGRAM

Adrián Colomer^{1,2}, Valery Naranjo^{1,2} and Jesús Angulo³

¹Instituto de Investigación e Innovación en Bioingeniería (I3B),

Universitat Politècnica de València, Camino de Vera s/n, 46022, Valencia, Spain.

²Grupo Tecnologas de Informática Aplicadas a la Oftalmología, Unidad Conjunta UPV-FISABIO, Spain.

³Centre de Morphologie Mathématique, Mathématiques et Systèmes,
MINES ParisTech, F-77305 Fontainebleau Cedex, France.

ABSTRACT

The high variability in fundus image databases is an important limiting drawback for detecting some retinal pathologies automatically. Age, human retinal pigmentation or lighting conditions affects in the colour of the acquired images. In this paper a colour-normalization method is presented as an initial pre-processing step in order to reduce the heterogeneity of retinal databases. The proposed method is based on geometric transformations applied to the chromaticity diagram of a target image taking into account a reference image. With the aim of quantifying the effect of the proposed colour normalization, a bright lesion detection from pathological images is carried out. A home-made system based on texture analysis and Support Vector Machine classification is used for this purpose. An improvement around a three percent in the detection accuracy demonstrates the importance of a retinal image colour pre-processing before any specific analysis. .

Index Terms— Colour-normalization, fundus images, exudates, LBP, SVM

1. INTRODUCTION

RGB retinal images are acquired through a retinal camera using non invasive protocols. This kind of images is commonly used by ophthalmologists in order to diagnosis some eye diseases. Diabetic retinopathy (DR) is one of the most frequent causes of blindness and vision impairment in the world [1]. The early diagnosis of this pathology is very important. However, due to the large population at risk, a potential automatic screening would highly benefit to clinicians.

Different fundus databases are publicly available, this fact is really helpful in the process of developing automatic models able to detect or classify pathological patterns extracted from the retinal images. The problem in this field is the high heterogeneity among images due to different factors.

The resolution of the images belonging to a specific database can be different due to the configuration of the retinal camera. Artefacts and noisy images (Fig.1a and Fig.1b) are really common in

This work was supported by the Ministerio de Economía y Competitividad of Spain, Project ACRIMA (TIN2013-46751-R). The work of Adrián Colomer has been supported by the Spanish Government under the FPI Grant BES-2014-067889. In particular, this work was developed at Centre for Mathematical Morphology belonging to the MINES ParisTech, PSL Research University, under the mobility grant EEBB-I-16-11276.

the databases due to the uncalibrated acquisition process. A non-uniform illumination in the image is propitiated by the different lighting conditions in the acquisition rooms. Besides the problems in the acquisition process, the retina variability can produce differences in the images such as highlights near the vessels characteristic of young retinas (Fig.1c) and the fundus colour that depends on age, ethnicity, differences in retina pigmentation and other anatomical human factors (Fig.1d).

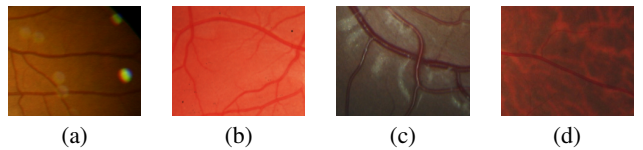


Fig. 1. Typical inconveniences in fundus databases. (a) Noisy images, (b) Images with artefacts, (c) Highlighted retina, (d) Tesselated images due to different ethnicity.

The factors described above are important for the success and reliability of the computer aided diagnosis of retinal pathologies. Previously to apply algorithms able to detect the pathology under study, a database normalization is an essential step in order to analyse the images in the same conditions.

Image pre-processing methods applied to fundus images have been studied in the literature. In [2] basic pre-processing techniques such as contrast adjustment, adaptive histogram equalization, median filtering and average filtering are applied before glaucoma detection. In most of the state-of-the art works [2–5], the non-uniform illumination is the main correction explored. However, the colour information have not been deep studied in this kind of images and it is necessary because the colour allows the visual discrimination of the different structures and lesions. For this reason, fundus images must be colour-normalized in order to be able to compare images belonging different patients and acquisition devices. In [5] a colour normalization based on histogram equalization and shape matching is applied on each RGB component separately with the aim of detecting the retinal anatomy.

In this paper, a chromatic colour-normalization involving the three RGB components is proposed. In this novel method, different geometric transformations are applied to the chromaticity diagram extracted from the images to be corrected. In order to test the performance of the proposed colour-transformation a bright lesion detection is carried out in DR images using a home-made system based on texture analysis and Support Vector Machine classification.

The rest of the paper is organized as follows: in Section 2 the proposed colour transformation is detailed and the procedure for its validation is described. Then, in Section 3 the obtained results for several tests using different pre-processing configurations are reported and discussed. Finally, Section 4 provides conclusions and some future work lines.

2. METHODS

2.1. Colour transformation

Let $I_i = (R_i, G_i, B_i)$ be a colour fundus image, we can obtain a luminance normalization as follows:

$$I_{i_norm} = \left(\frac{R_i}{L_i}, \frac{G_i}{L_i}, \frac{B_i}{L_i} \right) = (r_i, g_i, b_i) \quad (1)$$

with $L_i = R_i + G_i + B_i$.

From the normalized channels r_i and g_i a representation of the 2D histogram can be performed, the chromaticity diagram or chromatic distribution (CHD). In Fig.2 is possible to observe the CHD of the image I_i . The centre $c_i(c_{ri}, c_{gi})$ of this CHD is given by the coordinates of the maximum histogram value. This dominant mode of the chromatic distribution is associated to the colour of the retinal background. Also, we can compute the angle (θ_i) formed by the major axis of the fitted ellipse to the CHD and the horizontal axis (Fig.2).

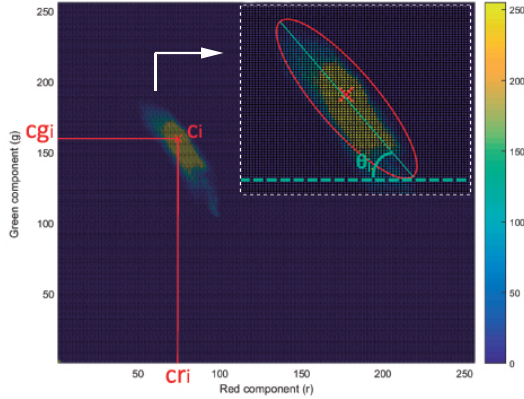


Fig. 2. Chromaticity diagram from a fundus image and visual description of $c_i(c_{ri}, c_{gi})$ and θ_i parameters.

The colour transformation of the target image I_i , taking as reference the image I_{ref} , is carried out in two steps. in the first one, a rotation of the CHD is applied, according to:

$$\begin{bmatrix} r'_i \\ g'_i \end{bmatrix} = \begin{bmatrix} r_i & g_i \end{bmatrix} \begin{bmatrix} \cos(\Delta\theta) & -\sin(\Delta\theta) \\ \sin(\Delta\theta) & \cos(\Delta\theta) \end{bmatrix} \quad (2)$$

where $\Delta\theta$ is the difference between the theta angle extracted from the target image to be transformed (θ_i) and the theta angle computed from the reference image (θ_{ref}).

In a second step, a translation of the centre of the CHD is performed following this equation:

$$\begin{bmatrix} r''_i \\ g''_i \end{bmatrix} = \begin{bmatrix} r'_i \\ g'_i \end{bmatrix} - \begin{bmatrix} \Delta c_r \\ \Delta c_g \end{bmatrix} \quad (3)$$

where $\Delta c_r = c_{ri} - c_{ref}$ being c_{ri} the red coordinate belonging to the centre of the CHD extracted from the image to be corrected and c_{ref} the red coordinate belonging to the centre of the CHD extracted from the reference image. In the same way, $\Delta c_g = c_{gi} - c_{gref}$ where c_{gi} indicates the green coordinate of the CHD centres.

After the colour transformation, the components r''_i and g''_i must be denormalized using the following equations:

$$b''_i = 1 - r''_i - g''_i \quad (4)$$

$$\tilde{I}_i = (r''_i L_i, g''_i L_i, b''_i L_i) = (\widetilde{R}_i, \widetilde{G}_i, \widetilde{B}_i) \quad (5)$$

Finally, the $\widetilde{R}_i, \widetilde{G}_i, \widetilde{B}_i$ components are the output of the colour transformation process detailed graphically in Fig.3. In this figure it is possible to observe the rotation and the translation operations applied to the CHD extracted from a target image taking into account a reference image.

2.2. Evaluation of the colour transformation method

With the aim of quantifying the improvement of using the proposed colour transformation method, a system based on texture analysis is used in order to distinguish between healthy and pathological areas from retinal images. In this section, the developed method to detect bright lesions (exudates) in fundus images is detailed.

2.2.1. Image pre-processing

First of all, a spatial normalization of the images [6] is carried out because fundus images belonging to the same database may present different resolution and in some cases retinal structures and lesions are not comparable. Taking into advantage the same capture angle (field of view) set in the acquisition process, it is possible to compute a resizing factor as $RF = D_{ref}/D_i$, where D_{ref} is a fixed reference diameter of the field of view and D_i is the image diameter to be resized.

Previous to the texture analysis stage, a blood vessel removal is performed as pre-processing step in the algorithm. The process of distinguishing between the healthy and the pathological texture could be hindered by the blood vessels. For this reason, inpainting techniques [7] are applied in order to remove them by diffusion-based methods.

2.2.2. Texture analysis

Texture analysis is performed locally, in other words, the image is divided in patches using a sliding window and texture descriptors are computed for each patch. The window used is a square of canonical size with an overlap of $(\Delta x, \Delta y)$.

Local Binary Patterns (LBP) is a grey-scale texture descriptor that establishes a label for each pixel taking into account its neighbourhood:

$$LBP_{P,R} = \sum_{p=0}^{P-1} s(g_p - g_c) \cdot 2^p, \quad s(x) = \begin{cases} 1 & \text{if } x \geq 0 \\ 0 & \text{if } x < 0 \end{cases} \quad (6)$$

where P represents the number of samples on the symmetric circular neighbourhood of radius R , the g_c is the gray value of pixel (i, j) and g_p the gray value of each neighbour. Note that the final assigned label is the decimal value of the binary word.

Many variants of LBP exist in the literature but the rotation-invariant uniform LBP presented in [8] is used in this work to encode a selected subset of patterns. When LBP is used for texture

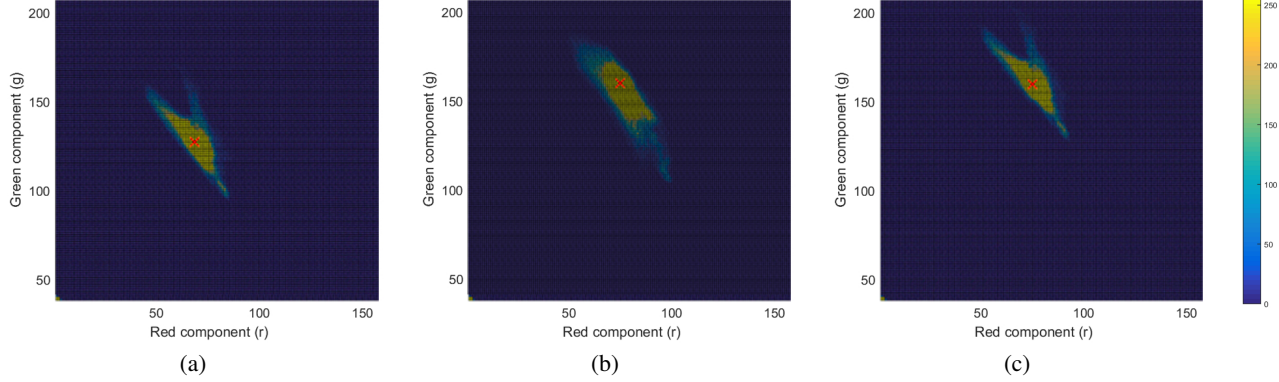


Fig. 3. Colour normalization process by linear transformation of chromatic histograms. (a) CHD from the image to be colour-transformed, (b) CHD from the reference image (c) CHD from the resulting image.

description it is common to include a contrast measure by defining the Rotational Invariant Local Variance (VAR) as:

$$VAR_{P,R} = \frac{1}{P} \sum_{p=0}^{P-1} (g_p - \mu)^2, \quad \mu = \frac{1}{P} \sum_{p=0}^{P-1} g_p \quad (7)$$

In this work, LBP and VAR are combined resulting the LBP variance (LBPV) [9]. Both descriptors are computed for the whole image and the normalized histogram of the LBPV is extracted from each patch. LBPV histogram accumulates the VAR value for each LBP label inside the window.

Colour information is extracted computing the LBPV descriptor for each channel of the RGB image and appending the normalized histograms in order to generate the feature vector.

2.2.3. Machine Learning techniques

After the feature extraction stage, the Support Vector Machines with Radial Basis Function (RBF-SVM) classifier [10] using the Bootstrap Aggregating (Bagging) technique [11] is utilized to classify each patch, extracted from an image, in healthy or pathological. SVM maximises the distance between the hyperplanes defined by the support vectors with the aim to find the optimal separation between classes. Combining the SVM method with the Bagging technique it is possible to improve the stability and accuracy of the machine learning algorithm, reducing the variance and avoiding the overfitting. In addition, in this work the Bagging technique is used to solve the problem of the unbalanced classes caused by the different number of healthy and pathological patches extracted from a fundus image. Given N pathological patches and K healthy patches where $K >> N$, the bagging technique can be applied in order to balance the classes. In first place, a random permutation of the healthy patches is carried out. After that, different SVM models can be trained using groups of N healthy patches and the N pathological patches. The final number of classifiers can be calculated as $M = \text{round}(K/N)$.

Note that in the test stage, each SVM classifier predicts one label for each patch and the final decision is obtained using a voting algorithm. In this work, the individual decision of each classifier is pondered by the probability assigned in the classification (weighted voting algorithm).

3. RESULTS

The validation of the proposed method was carried out on E-OPHTHA public database [12]. This database is divided in two subsets depending on the lesion type: exudates and microaneurysms. These lesions are manually annotated by experts. The subset of retinal images used to validate the colour-transformation method is composed by forty-seven images with exudates. The fundus images can present different resolutions (Table 1), for this reason the spatial normalization is essential.

Image resolution (pixels)	Number of images
2048 × 1360	9
2544 × 1696	23
1440 × 960	13
1504 × 1000	2

Table 1. Distribution of the E-OPHTHA images with exudates according to their resolution.

3.1. Colour-transformed images

In this work, the objective of the introduced colour normalization method is to reduce the high colour variability between images belonging to the same database. In order to quantify this fact, the images with exudates from the E-OPHTHA database were colour-transformed according to a reference image selected from this database. The reference image should be acquired using the appropriate protocol to capture fundus images with good illumination conditions and without special anatomical characteristics (as highlights, tessellations, etc.). Figure 4 shows several original images (b-g) and its corresponding colour transformation (h-m) taking as reference the image displayed in Fig.4a.

3.2. Exudate detection

The system explained in the section 2.2 was used in order to study if the lesion identification from colour-transformed images (reducing the heterogeneity in the database) is more efficient than the lesion detection from the original images. The forty-seven images of *E-OPHTHA exudates* database was divided in $s = 5$ partitions. External cross validation, using the “leave-one-out” technique, allowed

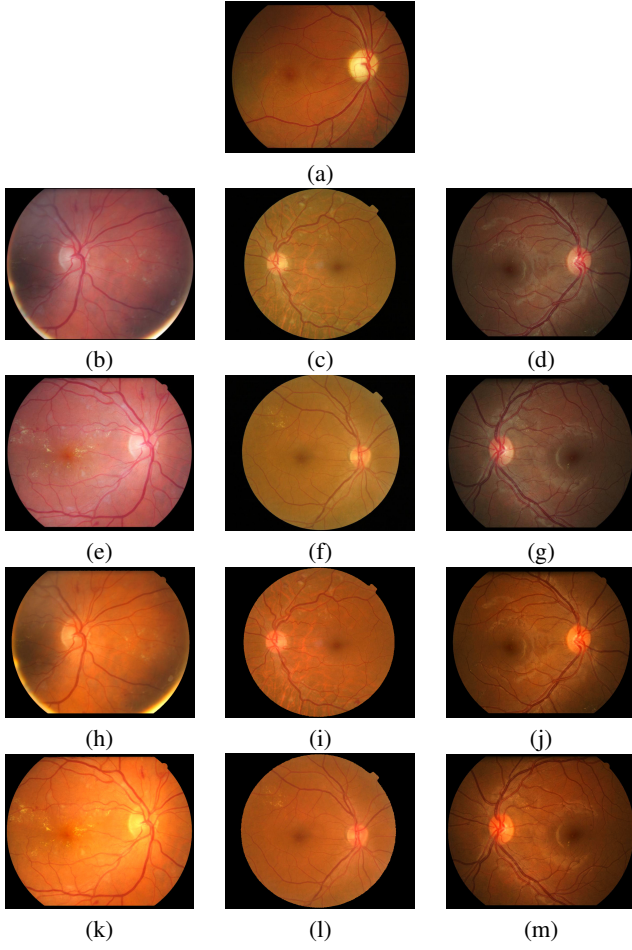


Fig. 4. Colour normalization results. (a) Reference image, (b-g) original images and (h-m) colour transformed images.

us to carry out a fair validation of the propose method. Tunable parameters involved in the process were set according to the Table 2. Notice that the optimal patch size, the overlap (Δx , Δy) used to extract the local features and the “cost” and “length-scale” parameters in SVM were obtained through internal cross validation with $t = 8$ folds.

	Spatial Norm.	Local analysis	LBP	Classification
Parameters	$D_{ref}=700$	Patch size=64 $\Delta x=\Delta y=32$	$R=1$ $P=8$	RBF kernel $M=5$

Table 2. Tunable parameters involved in the different stages of the lesion detection system.

Several tests using the original images (OI) and the colour-transformed images (CTI) applying the inpainting technique to remove the blood vessels (without vessels - WOV) and avoiding this step (with vessels - WV) were carried out. Table 3 shows the Area Under ROC Curve (AUC), accuracy, sensitivity and specificity of the resulting classification processes, taking into account the Ground-Truth provided by the ophthalmologists. Notice that for each classifier, we select a decision threshold γ obtaining the best

trade-off between sensitivity and specificity with the aim of reducing the effect of the unbalanced testing set.

	OI-WV	CTI-WV	OI-WOV	CTI-WOV
AUC	0.8017	0.8174	0.8388	0.8579
Accuracy	0.7352	0.7533	0.7713	0.8056
Sensitivity	0.7343	0.7561	0.7716	0.7949
Specificity	0.7531	0.7504	0.7808	0.7844

Table 3. AUC, accuracy, sensitivity and specificity related to the exudate detection for E-OPHTHA database taking into account different inputs: original image (OI-WV), colour-transformed image (CTI-WV), original image without vessels (OI-WOV) and colour-transformed image without vessels (CTI-WOV).

As can be observed in Table 3, the exudate detection is more accurate when pre-processing methods are applied to the original image. In particular, the accuracy increases 5% when inpainting techniques are applied in order to remove blood vessels. In addition, when the proposed colour normalization technique is carried out, the improvement in the accuracy of the lesion detection is about 3%. The mean ROC curves for each test are plotted in Fig. 5. As can be observe, CTI-WOV outperforms all of the explored pre-processing configurations for both, high and low false positives rates.

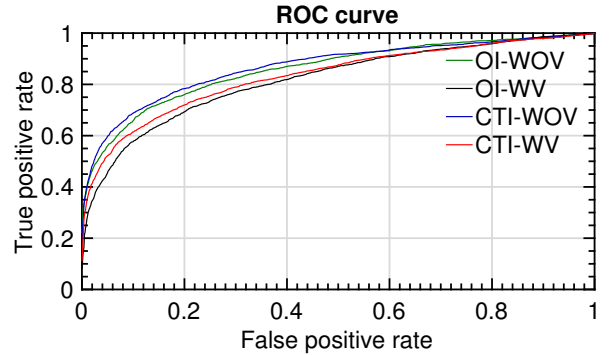


Fig. 5. ROC curves for the different tests.

4. CONCLUSIONS

In this work, a colour normalization method based on linear geometric transformations of the chromaticity diagram is proposed. From two geometrical parameters: the centroid associated to the r-g chromatic histogram and the angle formed by the major axis of the fitted ellipse to the CHD with the horizontal axis. In order to measure the effect of employing normalized fundus databases instead the original ones, a system based on texture analysis is used to detect bright lesions from the diabetic retinopathy images of *E-OPHTHA exudates* database. The results demonstrate the need to establish a colour normalization in order to homogenize the wide variability due to factors as the acquisition protocol or the human physiology.

In future work, the validation of the proposed method will be performed detecting another kind of lesions in diabetic retinopathy images. Microaneurysms and haemorrhages (dark red lesions) will be detected on the original and colour-transformed images from additional databases.

5. REFERENCES

- [1] World Health Organization (WHO), “Action plan for the prevention of avoidable blindness and visual impairment 2009–2013,” Tech. Rep., 2010.
- [2] S. Rathinam and S. Selvarajan, “Comparison of image processing techniques on fundus images for early diagnosis of glaucoma,” *International Journal of Scientific & Engineering Research*, vol. 4, no. 12, pp. 1368–1372, 2013.
- [3] J. Meier, R. Bock, G. Michelson, L.G. Nyúl, and J. Hornegger, *Effects of Preprocessing Eye Fundus Images on Appearance Based Glaucoma Classification*, pp. 165–172, 2007.
- [4] A. Marrugo and M. San Millán, “Retinal image analysis: preprocessing and feature extraction,” *Journal of Physics: Conference Series*, vol. 274, no. 1, pp. 012039, 2011.
- [5] Y. Aliaa, G. Atef, and G. Amr, *A Comparative Evaluation of Preprocessing Methods for Automatic Detection of Retinal Anatomy*, pp. 24–30, 2007.
- [6] X. Zhang, G. Thibault, E. Decencière, et al., “Spatial normalization of eye fundus images,” in *ISBI 2012 : 9th IEEE International Symposium on Biomedical Imaging*, Barcelone, Spain, 2012, IEEE.
- [7] C. Guillemot and O. Le Meur, “Image inpainting: Overview and recent advances,” *IEEE Signal Processing Magazine*, vol. 31, no. 1, pp. 127–144, 2014.
- [8] T. Ojala, M. Pietikainen, and T. Maenpaa, “Multiresolution gray-scale and rotation invariant texture classification with local binary patterns,” *IEEE Transactions on Pattern Analysis and Machine Intelligence*, vol. 24, no. 7, pp. 971–987, 2002.
- [9] Z. Guo, L. Zhang, and D. Zhang, “Rotation invariant texture classification using {LBP} variance (lbpv) with global matching,” *Pattern Recognition*, vol. 43, no. 3, pp. 706 – 719, 2010.
- [10] C. Chang and C. Lin, “Libsvm: A library for support vector machines,” *ACM Trans. Intell. Syst. Technol.*, vol. 2, no. 3, pp. 27:1–27:27, May 2011.
- [11] L. Breiman, “Bagging predictors,” *Machine Learning*, vol. 24, no. 2, pp. 123–140, 1996.
- [12] E. Decencière, G. Cazuguel, X. Zhang, G. Thibault, et al., “Teleophta: Machine learning and image processing methods for teleophthalmology,” *{IRBM}*, vol. 34, no. 2, pp. 196 – 203, 2013.